RESILIENT INFRASTRUCTURE
June 1–4, 2016
RESILIENT INFRASTRUCTURE LONDON 2016

SEISMIC RETROFIT OF EXISTING LOW-RISE STEEL BUILDINGS IN EASTERN CANADA USING ROCKING BRACED FRAME SYSTEM

Robert Tremblay
Polytechnique Montreal, Canada

Paul Mottier
Polytechnique Montreal, Canada

Colin Rogers
McGill University, Canada

ABSTRACT

A promising retrofit strategy consists of allowing deficient braced frames to rock at their bases to reduce the force demands on the structure and the foundation. For low-rise buildings, modifications to the structure may be limited to the braced frames, which then represent a very effective solution when compared to other approaches where alterations are needed along the entire lateral load path. In the article, the rocking braced frame solution is investigated for the seismic retrofit of 3-storey typical office buildings designed in accordance with codes prevailing in the early 1980s. The frames are located in Montreal, QC, and firm ground and soft soil conditions are examined for both locations. Rocking braced frames with friction energy dissipation mechanism are investigated. The response of the retrofitted structures is examined through nonlinear time history analyses using site representative ground motions and the results are compared to predictions from simplified models assuming first mode response.

Keywords: Brace steel frames, Earthquakes, Rocking, Uplift

1. INTRODUCTION

In Canada, special design and detailing requirements for ductile seismic response were introduced for the first time in 1989 in the CSA S16 steel design standard (Redwood and Channagiri 1990). Structures designed prior to this change to the steel design standard may not possess sufficient ductility to accommodate the inelastic deformations resulting from the reduced seismic design loads prescribed in the National Building Code of Canada (NBCC). Furthermore, seismic design provisions in the NBCC have evolved considerably in the last decades (Mitchell et al. 2010). In particular, design seismic loads specified for steel braced frames in the 1970-1985 code editions were significantly lower than those prescribed today (Figure 1a).

One approach to reduce the seismic forces transmitted to structures is to use controlled rocking response (Huckelbridge 1977, Priestley et al. 1978). For steel braced frames, this can be achieved by allowing braced frame columns to uplift at their bases (Figure 1b). Resistance to overturning can be provided by gravity loads supported by the frame acting in combination with added elastic post-tensioning (PT) and energy dissipating (ED) systems. The properties of the PT and ED systems can be adjusted to control lateral displacements while limiting force demands on members and foundations. Rocking systems are also expected to sustain minimal structural damage and exhibit self-centering response, which represent significance advantages in terms of cost and downtime periods after an earthquake. The response of the system has been verified experimentally for steel braced frame structures (e.g., Tremblay et al. 2008, Pollino and Bruneau 2010, Wiebe 2013). The system however presents limitations and drawbacks. In particular, base rocking is less effective for tall multi-storey buildings as large shear forces can still develop over the structure height (Tremblay et al. 2008). The beneficial effects of base rocking on overturning moments also reduce in the upper floors (Wiebe et al. 2013). Rocking is therefore expected to be more efficient for low-rise building applications. In eastern Canada, ground motions are expected to impose limited displacement

demands on structures (Tremblay and Atkinson 2001) and rocking system that do not include PT and ED systems may represent a viable solution for this part of the country. This article evaluates the potential of using gravity-based rocking braced frames for the seismic retrofit of seismically deficient low-rise steel buildings designed prior to 1990s in eastern Canada. The study is performed for a three-storey prototype building with steel braced frames located in Montreal, QC. Attention is paid to the computer analysis model used for the analysis.

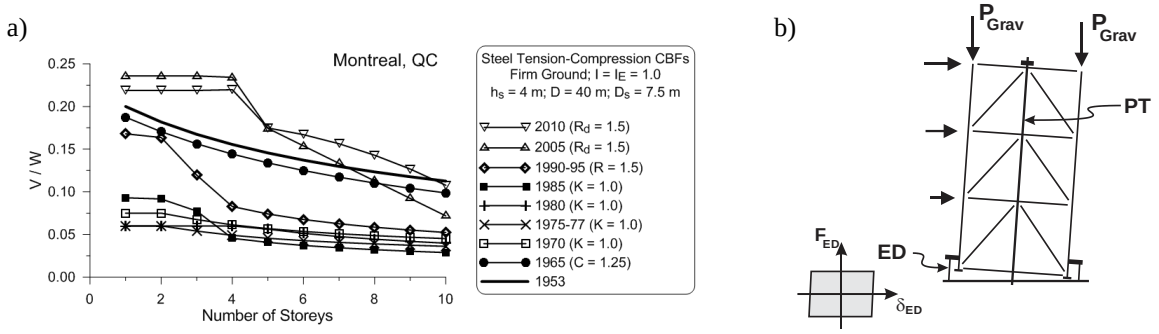

Figure 1: a) Evolution of seismic design forces in the NBCC; b) Rocking braced frame.

2. PROTOTYPE BUILDINGS

The structures studied are three-storey office buildings located in Montreal, QC. Site classes C (soft rock or firm ground) and E (soft soils) were considered to examine possible effects of the ground motion signature on rocking response. The plan dimensions of the two buildings were adjusted to obtain the same braced frame design for both site categories. The structures plan views, braced frame elevation and design gravity loads are given in Figure 2. The seismic force resisting system (SFRS) includes chevron braced frames in each of the four perimeter walls. Seismic resistance in the E-W direction is investigated herein. Light steel framing consisting of 38 mm deep steel deck panels placed on regularly spaced open web steel joists supported on steel girders are used at roof and floor levels. The floor slabs are 102 mm thick (38+63 mm) composite slabs. As shown in the figure, a closer joist spacing is used at the roof level. The braces are cold-formed square HSS members made from CSA G40.21-350W steel and columns and beams are W shapes with CSA G40.21-300W steel, as was the practice in the early 1980's.

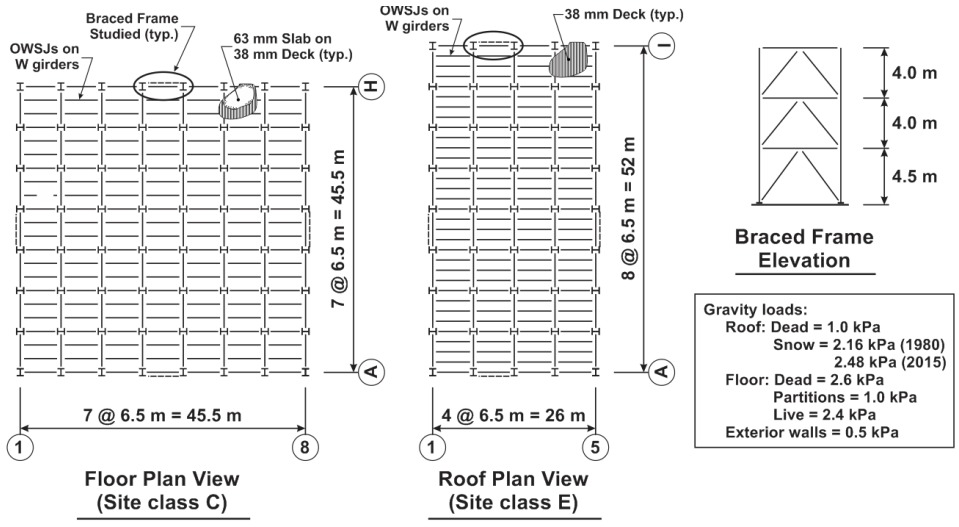

Figure 2: Prototype buildings studied.

2.1 Design of the prototype buildings

The structures were designed using the 1980 NBCC (NRCC 1980) and CSA S16.1-M78 steel design standard (CSA 1978). In the NBCC 1980, the minimum earthquake lateral design load, V, was given by:

[1] $V_{1980} = ASKIFW$

, where A was the design acceleration ratio, S was the seismic response factor, K was a coefficient that depended on the type of construction, F was the foundation factor, I was the importance factor, and W was the seismic weight. The design acceleration ratio A corresponded to peak ground accelerations established for a return period of 100 years and took a value between 0 and 0.08 depending on the seismic zone. For Montreal, A = 0.04 was specified. The factor S was equal to 1.0 but could be limited to 0.5/T0.5, where T was the fundamental period of the structure. For steel braced frames, T was given by: $T = 0.09h_n/D^{0.5}$, where h_n is the building height (12.5 m) and D the building dimension parallel to the loading direction. Lateral resistance along the E-W direction is considered herein and D = 45.5 m in that direction, which gives a period T = 0.17 s and, thereby, S = 1.0. It is noted that S in the 1980 NBCC could also be determined using the period computed from methods of mechanics, without any prescribed upper limit. However, this relaxation was intended for tall buildings and was generally not used for low-rise buildings. The K factor varied from 0.7 for the most ductile seismic force resisting systems (e.g., ductile moment-resisting space frames) to 2.0 for the least ductile ones (unreinforced masonry). The vertical bracing is composed of tension-compression chevron bracing for which a value of 1.0 was specified for K. For buildings of normal importance, I was equal to 1.0 and the factor F was equal to 1.0 for rock and firm ground sites and 1.5 for soft soil conditions. The seismic weight included the dead load plus 25% of the design roof snow load. In NBCC 1980, the roof snow load for Montreal was 2.16 kPa. Using these values in Equation 1, the original design seismic load V_{1980} for both structures studied is equal to 761 kN. Two load combinations with earthquake loads were considered in the 1980 code: 1.25D + 1.5E and 1.25D + 0.7(1.5L + 1.5E), where L included the snow load. Hence, for the design of SFRS components, 1.5 E was used, given a factored seismic load $V_{f,1980} = 1.5 \times 761 = 1142$ kN. For simplicity in this study, accidental torsional effects were ignored. The equivalent static equivalent force procedure was used for distributing the seismic loads over the building height and storey shear per braced frames are given in Table 1. The design was performed to achieve minimum steel tonnage. The brace factored compression loads $C_{df,1980}$ and selected bracing members are given in the table. This design applies to both site conditions as the building dimensions were adjusted to obtain the same member forces. The columns are W200x46 over the entire building height. For the building on site class C, the periods in modes 1 to 3 are 0.81, 0.37 and 0.26 s, respectively. For site class E, the corresponding values are 0.71, 0.29 and 0.20 s.

Table 1: Seismic design and evaluation of the bracing members (forces / braced frame)

Level	$V_{f,1980}$ (kN)	$C_{df,1980}$ (kN)	Bracing members	$C_{dr,1980}$ (kN)	$V_{f,0.6x2015}$ (kN)	$C_{df,0.6x2015}$ (kN)	$C_{dr,2015}$ (kN)	$C_{dn,2015}$ (kN)
3	167	136	HSS102x102x4.8	158	239	193	185	205
2	431	360	HSS152x152x4.8	444	430	358	502	568
1	571	507	HSS152x152x6.4	516	569	504	598	662

2.2 Seismic evaluation of the prototype buildings

According to NBCC, existing building structures are evaluated using 60% of the design seismic loads prescribed in the current building code. In the NBCC 2015, the minimum earthquake load V is given by:

[2] $$V_{2015} = \frac{S(T_a) M_v I_E W}{R_d R_o}$$

where S is the design spectrum, T_a is the structure fundamental period used in design, M_V is a factor that accounts for higher mode effects on base shear, W is the seismic weight and R_d and R_o are ductility- and overstrength-related force modification factors. The design spectrum is obtained from uniform hazard spectral ordinates S_a that are specified at periods of 0.2, 0.5, 1.0, 2.0, 5.0 and 10 s and modified by site factors F(T) to account for local site

conditions. The resulting design spectra at both sites are given in Figure 3. The F factors at periods of 0.2, 0.5, and 1.0 s are respectively equal to 1.048, 1.477, and 1.737, which is different from the unique value of 1.5 in NBCC 1980. The period T_a can be taken as the building fundamental period determined from analysis, without exceeding $T_a = 0.05\ h_n$. For the buildings studied, this upper limit controls and $T_a = 0.625$ s is used. The factor $M_v = 1.0$ for braced frames with periods less than 1.0 s. The importance factor I_E is also equal to 1.0. The seismic weight in the 2015 NBCC is same as in 1980 except that seismic weights at floor levels are determined using 0.5 kPa for the partition loads. In addition, the roof snow load for Montreal has increased to 2.48 kPa in 2015. The modified seismic weights are considered in the seismic evaluation as well as in the analyses of the rocking braced frame systems described later. The 1980 braced frame design was performed without any special design and detailing requirements for seismic ductility and the structures SFRS are considered as being of the Conventional Construction (Type CC) category with $R_d = 1.5$ and $R_o = 1.3$. In the 2015 NBCC, V from Equation 2 need not exceed the larger of 2/3 the value determined with $T_a = 0.2$ s and the value determined with $T_a = 0.5$ s.

Although the equivalent static force procedure is permitted for both buildings, dynamic (response spectrum) analysis was performed to better assess seismic demands. For regular structures such as the ones studied herein, the design base shear V_d from dynamic analysis is taken as the larger of 0.8V and V_eI_E/R_dR_o, where V_e is the base shear from analysis performed with the design spectra S. The analysis results are then multiplied by V_d/V_e. For the building on site class C, the periods in the first three lateral modes with the revised seismic weights are 0.87, 0.36 and 0.24 s. The upper limit on T_a (= 0.625 s) is used to determined S, which gives S = 0.270 and V = 2370 kN. For this structure, V_e from response spectrum analysis is equal to 2962 kN and V_d = 1896 kN (= 0.8V). For the structure on site class E, the computed periods T_1 to T_3 are 0.71, 0.29 and 0.20 s and the period $T_a = 0.625$ s is also used, which gives S = 0.408 and V = 2378 kN. The base shear V_e = 3712 kN, which leads to V_d = 1902 kN (= $0.8V \approx V_eI_E/R_dR_o$).

Values of 60% V_d for site classes C and E are 1138 and 1141 kN, which are coincidentally very close to the factored base shear used in 1980 (1142 kN), which suggests that seismic rehabilitation would not be triggered. In Table 1, detailed calculations are performed for the bracing members of the building on site class C. Storey shears and brace factored loads due to 60% NBCC 2015 seismic loads ($V_{f,0.6x2015}$ and $C_{df,0.6x2015}$) are given together with the braces factored compressive resistances determined with CSA S16-14 ($C_{dr,14}$). For $C_{dr,14}$, an effective length factor K = 0.9 was adopted to reflect the actual buckling length of the braces. As shown, $C_{df,0.6x2015}$ slightly exceeds $C_{dr,14}$ at the third level but is less than $C_{dr,14}$ at the other two floors. The columns at level 1 were also verified. From analysis, the factored axial compression load from gravity and 60% V_d is equal to 635 kN for the structure on site class C (640 kN for site class E) , which less than the factored compressive resistance of the column (877 kN). In spite of this positive assessment, seismic retrofit could be appropriate for these structures considering that CSA S16-14 now requires connections in Type CC SFRSs to either exhibit a ductile governing failure mode or be designed for forces amplified by $R_d = 1.5$. Non-ductile failure in tension on net section typically governs HSS brace connections and connections designed for loads close to $C_{fx,1980}$ in Table 1 would not satisfy the S16 required design load requirements. Furthermore, brace buckling will be expected under the NBCC 2015 seismic loads, and the resulting vertical unbalanced brace loads at beam mid-span could have detrimental impact on the frame response. A retrofit scheme aiming at limiting brace axial loads to the brace compressive strengths would therefore be desirable.

2.3 Rocking braced frame as a seismic retrofit strategy

The rocking braced frame retrofit strategy considered herein consists in simply removing the nuts of the anchor rods of the braced frame columns to allow uplift to occur. As shown in Figure 3a, horizontal reaction blocks would be anchored to the existing foundation on both sides of the braced frame to resist base shear forces acting in either direction. A horizontal strut connecting the two column bases would be added to transfer the horizontal component of the brace forces at the base of the uplifting columns to the opposite columns bearing against the reaction block. No vertical pretension would be used; however, a friction mechanism with slotted bolted connections would be mounted on each reaction block and connected to the adjacent column to dissipate seismic input energy and control the structure rocking response. Lateral and vertical forces acting on the braced frame upon rocking are illustrated in Figure 3b. Forces F_x are the horizontal inertia forces developing at every level x. The force F_s is the slip resistance of the energy dissipation (ED) system. Forces $P_{gc,x}$ represent the gravity loads supported by the braced frame columns (including loads applied to the braced frame beams). In the figure, a P-Δ column is added to include the effects on lateral response of the gravity loads $P_{gb,x}$ supported by the building columns laterally braced by the braced frame studied. Equilibrium of the vertical forces and moments give:

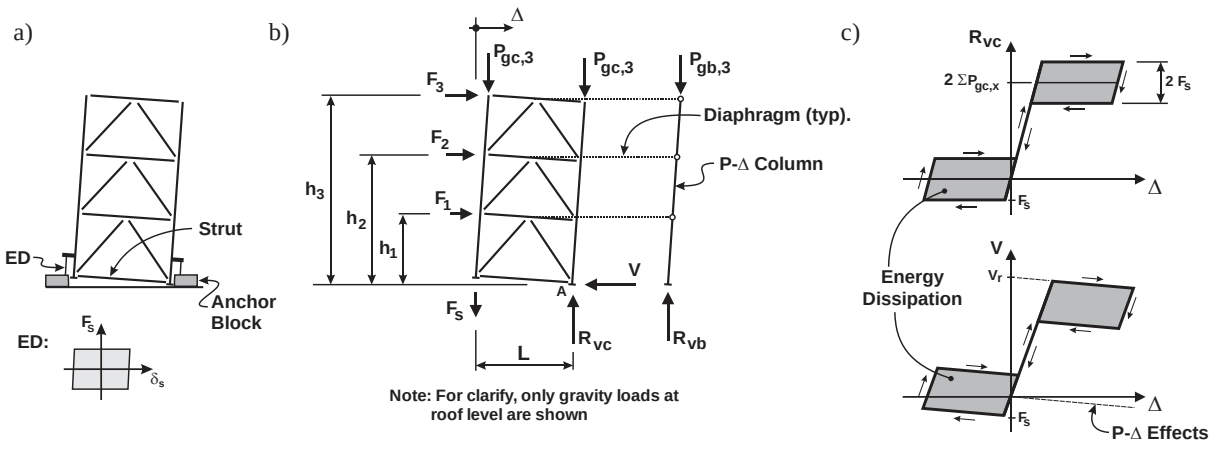

Figure 3: a) Rocking braced frame retrofit scheme; b) Forces upon rocking.

[3] $$R_{vc,max} = 2\sum P_{gc,x} + F_s$$

[4] $$\left(\sum P_{gc,x} + F_s\right) L = \sum F_x h_x + \sum\left(2P_{gc,x} + P_{gb,x}\right)\Delta_x$$

Equation 3 gives the maximum vertical reaction at the base of the column in contact with the foundation. When uplifting, column bases are subjected to a tension force equal to F_s. Assuming first mode response, lateral displacements Δ_x and accelerations are considered to vary linearly with the height of the levels above ground, h_x. Using this assumption, Equation 4 can be written as follows:

[5] $$V = \frac{\sum(W_x h_x)}{\sum\left(W_x h_x^2\right)}\left[\left(\sum P_{gc,x} + F_s\right) L - \frac{\Delta_n}{h_n}\sum\left(\left\{2P_{gc,x} + P_{gb,x}\right\} h_x\right)\right]$$

where V is the total lateral load that can be resisted by the rocking frame. The first term in this expression represents the resistance to uplift whereas the second term represents P-delta negative effects on lateral resistance. The total lateral load to trigger uplift can be estimated by setting $\Delta_n = 0$:

[6] $$V_r = \frac{\sum(W_x h_x)}{\sum\left(W_x h_x^2\right)}\left(\sum P_{gc,x} + F_s\right) L$$

Variations of R_{vc} and lateral load V with lateral displacement are illustrated in Figure 3c. In design, a larger slip load F_s results in higher energy dissipation capacity, which generally contributes to reducing frame lateral displacements. However, larger F_s values result in higher force demand on the members and F_s must be kept lower than the dead load carried by the braced frame columns to ensure self-centering response. For the braced frames studied, the reaction at the column basses due to dead, live, and snow loads are $\Sigma P_{gc,D}$ = 199 kN, $\Sigma P_{gc,L}$ = 101 kN, and $\Sigma P_{gc,S}$ = 52 kN. After a few trials, slip loads equal to 50 kN and 220 kN were selected for the buildings located on site classes C and E, respectively. The larger value required for site class E is due to the relatively larger displacement demand from ground motions in soft soils. Under the load combination D+0.5L+0.25S, the total column gravity load is 263 kN. From Equation 3, the total vertical reactions expected at the column bases are respectively 576 and 746 kN for the two sites. From Equation 6, the loads V_r at onset of rocking are equal to 228 and 352 kN per braced frame for the structures on site classes C and E, respectively. Upon rocking, lateral loads are expected to reduce with displacements due to P-Δ effects (Equation 5) and it is anticipated that lateral loads on the braced frames will not exceed V_r during ground motions. Values of $2V_r$ for the entire buildings (456 and 704 kN) represent fractions (40% and 61%) of the factored base shear design $V_{f,1980}$ = 1142 kN used in the original design. This suggests that the proposed rocking braced frame retrofit strategy could effectively protect members and connections of the existing braced frames from being overstressed during strong seismic ground motions.

3. SEISMIC RESPONSE OF THE PROPOSED ROCKING FRAMES

3.1 Numerical model and ground motions

Response history analysis was performed to study the response of the rocking braced frames under seismic ground motions and validate the predictions made in Section 2.3. The analyses were performed using the commercial SAP2000 computer software (CSI 2016). The program offers several nonlinear analysis capabilities including nonlinear link elements that can be introduced at the column bases to simulate rocking response with energy dissipation. Two different models were used in this study: Model P and Model M. The former is a simple 2D model of the rocking braced frame (Figure 4a). Gravity loads carried by the frame beams and columns are specified in the model. The model also includes a "P-delta" column to reproduce global P-delta effects on lateral response due to gravity loads P_{gb} described earlier. The P-delta column was modeled with truss elements and lateral displacements at every level were constrained to be same as those of the braced frame. Nonlinear links elements were used to represent the contact (Gap type) and friction energy dissipation (Multilinear type) at the column bases. Non-linear (P-delta) static analysis under the concomitant gravity loads was performed first. Nonlinear dynamic analysis was then carried out under the ground motion histories including gravity load effects from the previous static analysis. A direct integration (Newmark-Beta) scheme was used for the dynamic analysis and P-delta effects were included. Mass proportional damping corresponding to 3% of critical at the period associated to rocking response was assigned to the structure. In addition, stiffness proportional damping corresponding to 3% of critical in lateral modes 1 and 2 of the fixed base structures was assigned to the steel material of the beams and columns. Initial effective stiffness and damping properties were set equal to zero for the link elements to prevent fictitious damping forces at the column bases during rocking response.

Figure 4: Numerical models: a) 2D Model P; 3D Model M; and c) Floor beam vibration mode (from Model M).

Model M is a 3D model that includes all beams connecting to the rocking braced frames (Figure 4b). In the model, all gravity loads supported by these beams are specified as vertical masses to capture inertia forces and dynamic response developing in the vertical direction upon frame rocking. For the frames studied, the fundamental periods of vibration of the floor and roof beams are respectively equal to 0.32 and 0.21 s, respectively. Vertical load on the P-delta column are also specified as vertical masses. No static analysis under gravity loads was performed. Instead, downward vertical acceleration of 1.0 g, starting with a 4.5 s linear ramp, was applied at the same time of the ground motion histories so that gravity loads and P-delta effects were considered simultaneously in the analyses. Ground motion records were delayed by 5.0 s to start after the gravity loads have been entirely applied. Damping modelling and integration techniques were same as in Model P.

A suite of 11 simulated ground motion time histories was used for each site. The records were generated for magnitude-distance scenarios dominating the hazard at the sites, i.e. 5 records from M6.0 events at close distance and 6 records from M7.0 at longer distances, as well as the local site classes (Atkinson 2009). The ground motions were then scaled to match the design spectrum (Tremblay et al. 2015). The absolute response spectra of the scaled ground motions are shown in Figure 5a.

3.2 Overall frame response

Frame rocking response developed under all ground motions considered at both sites. Typical time histories of the roof lateral displacement (Δ_n) and column uplifts (w) obtained from Model M are illustrated in Figure 5b. As shown, the frame lateral response correlates well with column uplift and peak lateral displacements are mainly due to rocking response. For the case shown, maximum uplift of the LHS column is 53 mm, which would induce a roof lateral displacement of 102 mm assuming rigid frame response (= 53 mm × 12.5 m / 6.5 m). This value represents 85% of the roof displacement from analysis at the same time (120 mm = 0.96% h_n).

Statistics of key response parameters are given in Table 2 for the structures located at both site classes. The mean value, the mean value of the largest 5 values, the mean values of the largest 3 values and the maximum value of the peak results from the 11 ground motions of each suite are presented to assess variability in the response. The values in the table are those obtained from Model M. When available, values from Model P are given in brackets. As shown, mean values of the roof lateral displacements from Model M at both sites are less than the 1.0% h_n limit specified in NBCC 2015 for post-disaster buildings, which indicates that lateral deformations could be well controlled with the proposed retrofit solution. As shown, Model M generally gives smaller column uplifts and lateral displacements. This is attributed to vertical inertia forces developing at the roof and floor levels when columns uplift occurs. These inertia forces restrain upward displacements of the columns and, thereby, the rocking response of the frame. This restraining effect on roof lateral displacements can be seen in Fig. 5b when comparing results from Models M and P. Vertical acceleration effects are discussed further in the next section.

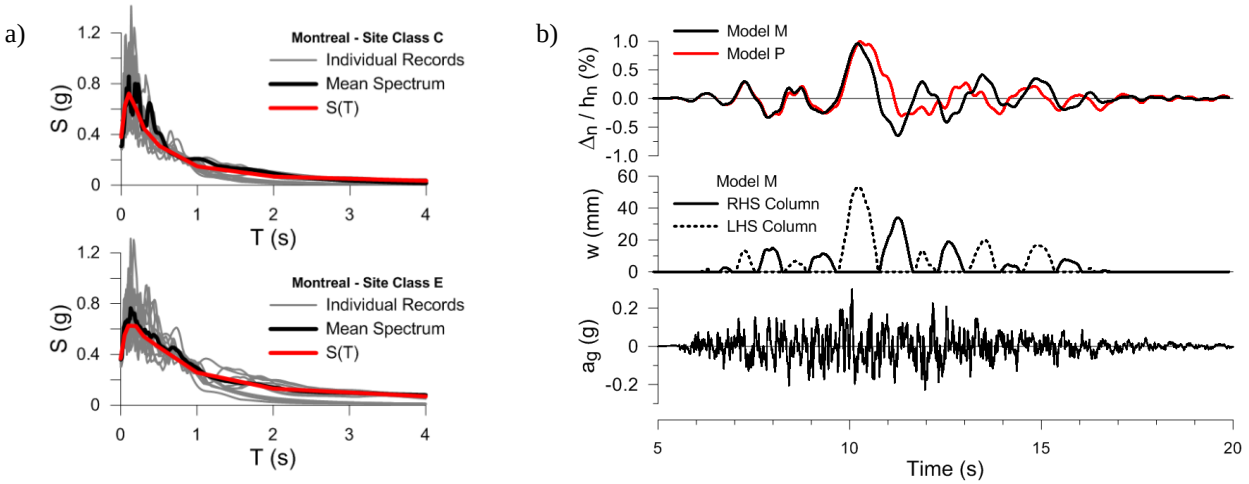

Figure 5 a) 5% damped acceleration spectra of the ground motions; b) Overall frame response for the structure on class C site under subjected to M7.0 at 42 km ground motion.

Table 2: Statistics of key response parameters from Model M (values from Model P are given in brackets)

	Montreal, Site C				Montreal, Site E			
Parameters	Mean	Mean of largest 5	Mean of largest 3	Maximum	Mean	Mean of largest 5	Mean of largest 3	Maximum
w (mm)	36 (45)	54 (70)	59 (76)	75 (90)	41 (47)	59 (76)	75 (90)	105 (132)
Δ_n (%h_n)	0.67 (0.79)	0.95 (1.16)	1.03 (1.25)	1.28 (1.44)	0.79 (0.85)	1.00 (1.14)	1.18 (1.35)	1.81 (2.15)
$R_{vc}/R_{vc,max}$	1.48 (1.00)	1.68 (1.00)	1.75 (1.00)	1.87 (1.00)	1.39 (1.00)	1.51 (1.00)	1.59 (1.00)	1.87 (1.00)
V/V_r	3.31 (3.10)	3.90 (3.85)	4.27 (4.24)	4.54 (4.62)	2.30 (2.07)	2.56 (2.31)	2.63 (2.44)	2.76 (2.51)
$C_{c,1}/C_{cn,1}$	0.84 (0.73)	0.93 (0.82)	0.93 (0.82)	1.08 (0.98)	0.87 (0.76)	0.93 (0.85)	0.93 (0.85)	0.97 (0.89)
$C_{d,3}/C_{dn,3}$	2.10 (2.16)	2.54 (2.64)	2.83 (3.01)	3.27 (3.27)	1.87 (1.89)	2.21 (2.31)	2.23 (2.42)	2.25 (2.55)
$C_{d,2}/C_{dn,2}$	0.69 (0.66)	0.78 (0.72)	0.81 (0.74)	0.84 (0.78)	0.85 (0.75)	0.81 (1.01)	0.86 (1.13)	1.13 (0.93)
$C_{d,1}/C_{dn,1}$	1.06 (0.97)	1.23 (1.19)	1.33 (1.30)	1.42 (1.42)	1.10 (1.00)	1. 21(1.11)	1.24 (1.16)	1.30 (1.20)
$a_{h,3}$ (g)	0.30	0.37	0.41	0.47	0.42	0.49	0.50	0.51
$a_{h,2}$ (g)	0.16	0.19	0.21	0.25	0.21	0.24	0.25	0.26
$a_{h,1}$ (g)	0.22	0.28	0.31	0.31	0.29	0.34	039	0.42
$a_{v,3}$ (g)	0.50	0.63	0.73	0.91	0.74	0.91	0.99	1.28

3.3 Base reactions and member forces

Time histories of the vertical reactions R_{cv} at both column bases, as obtained from Model M, are plotted in Figure 6a for the example discussed in Figure 5b. Only the 6-14 s portion of the response is shown on the graphs. The hysteretic response of the column base reaction *vs* roof displacement from both models are given in the upper part of Figure 6b. As expected, the reaction upon column lifting is equal to F_s in tension (= 50 kN for the case shown). When the column base returns to its initial position, the force F_s is reversed and maintained until contact is established with foundation. At the base of the supported column, the upward reaction reaches and exceeds the predicted $R_{cv,max}$ value in every rocking cycle. The peak amplitude of R_{cv} generally increases with the importance of the uplift excursion in the opposed column. The higher base reactions are caused by the downward inertia forces that develop at the roof and floor levels when columns uplift. These forces add to ΣP_{gc} and F_s in Equation 3 to resist rocking. Time histories of the vertical shear in the roof girder connecting to the RHS column ($V_{G,3}$) and the axial compression load at the third level of that column ($C_{c,3}$) are plotted in Figure 6a. At the beginning of the ground motion, these two forces are respectively equal to 34 kN and 45 kN, as predicted from statics. Once rocking response initiates, larger forces develop when the column moves upward due to the additional vertical inertia forces. In figure 6b, it is clear that these forces are not captured in Model P. As shown in Table 2, this dynamic amplification can be in the order of 1.4 to 1.9 depending on the probability level.

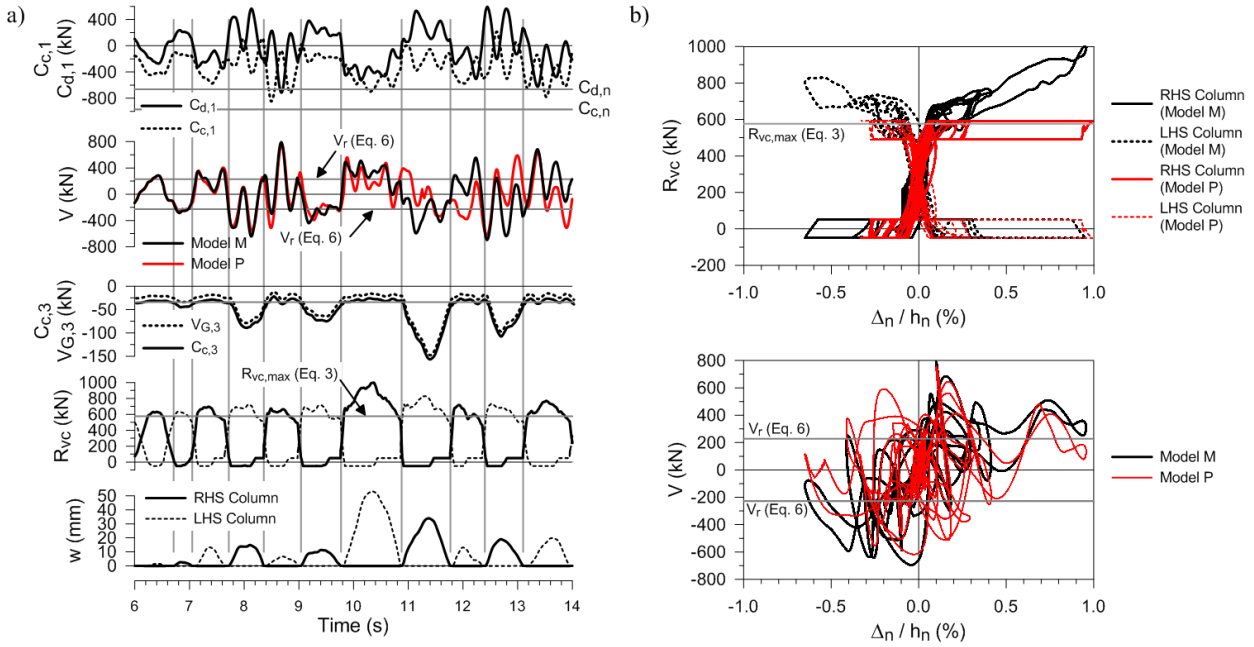

Figure 6: Response of the structure on class C site to M7.0 at 42 km ground motion:
a) Time histories of key response parameters; b) Vertical reaction and base shear hysteretic responses.

Base shear time histories from both models are plotted in Figure 6a, together with the predicted V_r upper limits predicted from Equation 6. For Model M, close examination of the base shear signal reveals a general correlation with the rocking (uplift) response as the base shear changes sign (or direction), on average, when the rocking response is reversed. During the large rocking excursions between 9 and 12 s, the average base shear amplitude is closer to the predicted V_r limits, although significant variations can be observed. These oscillations are more pronounced during the smaller rocking cycles. The period of these oscillations (0.3-0.4 s) is close to the second mode period of the fixed base structure, suggesting that higher mode response contributes to the frame lateral response. When comparing the bottom graphs of Figures 3b and 6b, it is clear that this higher mode demand has a profound impact on the base shear demand. As shown in Figures 6a and 6b, this behaviour is also observed when using Model P, which confirms that this additional contribution to base shear is dominated by higher lateral vibration modes. The history of the axial load in the brace at Level 1 that connects to the base of the RHS column is plotted in the uppermost graph of Figure 6a. The axial load in that column is also presented in the same plot. As expected, the brace axial load correlates nearly perfectly with the base shear response. Since vertical equilibrium

must be maintained at column bases, axial compression in the column is also affected by the structure higher mode response. For this particular example, the peak axial load in the brace exceeds the nominal compression resistance of the braces C_{dn} (= $C_{dr,14}$ / ϕ), meaning that the brace would have buckled under that particular ground motion. Conversely, the column nominal compressive strength C_{cn} is sufficient to prevent column buckling in that analysis. In Table 2, the values of V/V_r show that V_r significantly underestimates the base shear demands. Statistics of peak axial forces in the braces at all three levels and in the first-storey column are also given in the table. The retrofit scheme would adequately protect the column and the braces at the second level but the braces at the first and third levels would require strengthening if buckling limit states are to be avoided.

3.3 Acceleration demands

Peak values of the horizontal absolute accelerations ($a_{h,x}$) at every level are reported in Table 2. Examination of floor acceleration time history responses do not reveal clear correlation with frame rocking response. For both site classes, peak horizontal accelerations in the structures are larger at the third (roof) and first levels. The relatively lower accelerations computed at the second level confirm that the second translational mode of vibration of the structure dominates the seismic lateral force demands. Horizontal accelerations may cause damage to non-structural components in buildings. In the 2015 NBCC, peak accelerations for the design of non-structural components would be equal to 0.54 and 0.31g at the third and first levels of the structure on the class C site. The corresponding values in Table 2 are lower or comparable to these design values, which means that a rocking braced solution would not induce horizontal accelerations in excess of those assumed in current code provisions. Rocking response may however induce significant vertical accelerations of the floors and roof components affected by column uplift, as revealed by the peak vertical accelerations values computed at mid-span of the roof girder framing into the RHS braced frame column ($a_{v,3}$). In addition to the impact on column axial loads discussed earlier, these vertical accelerations may impose additional shear and moments demands in beams as well as extra shears on beam-to-column connections. This aspect must be considered when relying on gravity loads to control frame rocking response.

4. CONCLUSIONS

Hypothetical three-storey office buildings located on site classes C and E in eastern Canada were designed in accordance with the seismic provisions of the 1980 NBCC. Chevron bracing was selected for these structures and seismic evaluation using the 2015 NBCC seismic provisions revealed that the brace connections could be prone to brittle failure in the eventuality of a future strong earthquake. The rocking frames solely rely on the columns tributary gravity loads for self-centering response, rather than added vertical post-tensioning. Friction based energy dissipation is added to control rocking and lateral displacements. Assuming first mode lateral response, equations have been proposed to predict the maximum vertical reactions and horizontal shears at the base of the rocking frames. Nonlinear response history analysis was performed to examine the response of the rocking braced frames and propose recommendations for the use of this retrofit solution. In the analyses, gravity loads were modelled using vertical masses to reproduce possible vertical inertia forces and dynamic response induced by column uplift. A simplified model with gravity loads specified as forces was also used for comparison purposes. The following conclusions can be drawn from this study:

1. For the structures studied, rocking braced frames supporting gravity loads and equipped with friction energy dissipation were sufficient to achieve satisfactory column uplift and building lateral displacement responses. Lateral deformations could be predicted with some conservatism with a simplified numerical model without vertical masses.
2. Vertical inertia forces developed at the floor and roof levels due to column uplift response. Those resulted in higher vertical base reactions, amplified column axial loads and additional localized force demands on the floor and roof framing members and their connections. This increased force demand must be considered in design. Vertical inertia forces may also contribute to reducing the lateral displacements of the rocking frames. Vertical inertia forces and their effects can only be obtained in the analysis by modelling gravity loads on the form of vertical masses.
3. The equation proposed to predict maximum vertical reactions must include vertical acceleration effects.
4. Horizontal reactions at the structures bases correlated to some degree with the frame rocking response, but they were also significantly influenced by the higher lateral modes of vibration of the structures. Peak base shears

were markedly underestimated from simple equations based on commonly adopted first mode response assumptions. Brace axial forces and, to a lesser extent, column axial loads were also significantly influenced by the structure higher mode lateral response. Base shears and axial load demands on braces and columns can be predicted using numerical models without vertical masses.

5. Peak floor accelerations in the structures with rocking braced frames were comparable to those assumed in current codes for the design of non-structural components.

The dynamic seismic response of rocking braced steel frames that rely on gravity for self-centering response should be validated through physical testing. The study was limited to three-storey structures located in eastern Canada. Future studies should examine structures located in western Canada where larger seismic displacement demands are expected as well as two-storey structures for which higher mode demand should be reduced. Additional research should also examine alternative energy dissipation systems and bracing configuration with the objectives of reducing member forces and lateral displacements. Additional research should also aim at developing simple design guidelines and methods to achieve effective rocking braced frame designs in day-to-day practice.

ACKNOWLEDGEMENTS

Funding for this research was provided by the Fonds de recherche du Québec - Nature et technologies (FRQNT) of the Government of Quebec, Canada.

REFERENCES

CSA. 1978. *CAN3-S16.1-M78, Steel Structures for Buildings – Limit States Design*. Canadian Standards Association (CSA), Rexdale, ON, Canada.

Huckelbridge, A. A. 1977. *Earthquake simulation tests of a nine story steel frame columns allowed to uplift*. Report no. UCB/EERC-77/23, Earthquake Engineering Research Center, University of California, Berkeley, CA, USA.

Mitchell, D., Paultre, P., Tinawi, R., Saatcioglu, M., Tremblay, R. Elwood, K., Adams, J., and DeVall, R. 2010. Evolution of Seismic Design Codes in Canada. *Canadian Journal of Civil Engineering*, 37 (9): 1157-1170.

NRCC. 1980. National Building Code of Canada (NBCC), 8th ed., National Research Council of Canada (NRCC), Ottawa, ON, Canada.

NRCC. 2015. National Building Code of Canada (NBCC), Draft December 2015, Standard Committee on Earthquake Design, National Research Council of Canada (NRCC), Ottawa, ON, Canada.

Pollino, M. and Bruneau, M. 2010. Seismic Testing of a Bridge Steel Truss Pier Designed for Controlled Rocking. *Journal of Structural Engineering*, 10.1061/(ASCE)ST.1943-541X.0000261, 1523-1532.

Priestley, M. J. N., Evison, R. J., and Carr, A. J. 1978. Seismic response of structures free to rock on their foundations. *New Zealand National Society for Earthquake Engineering Bulletin*, 11 (3), 141-150.

Redwood, R.G., Channagiri, V.S. 1990. Earthquake resistant design of concentrically braced steel frames. *Canadian Journal of Civil Engineering*, 18 (5): 839-850.

Tremblay, R., Poirier, L.-P., Bouaanani, N., Leclerc, M., René, V., Fronteddu, L., and Rivest, S. 2008. Innovative viscously damped rocking braced steel frames. *Proceeding 14th WCEE, Beijing*, China, Paper No. 05-01-0527.

Wiebe, L., Christopoulos, C., Tremblay, R., and Leclerc, M. 2013. Mechanisms to limit higher mode effects in a controlled rocking steel frame. 1: Concept, modelling, and low-amplitude shake table testing, 2: Large-amplitude shake table testing. *Earthquake Engineering and Structural Dynamics*, 42 (7), 1053-1086.